Glycoconjugate Journal (2026) 43:1
https://doi.org/10.1007/s10719-025-10202-0

RESEARCH

Identification of a distinct sialic acid (KDN) and a KDN-specific aldolase in Pacific oyster

Zi-Xuan Hu[1] · Jia-Yu Zhang[1] · Jitske van Ede[2] · Yao-Yao Zhang[1] · Yu-Quan Li[1] · Mattia Ghirardello[3] · M. Carmen Galan[4] · Martin Pabst[2] · Li Liu[1] · Josef Voglmeir[1]

Received: 7 July 2025 / Revised: 23 October 2025 / Accepted: 27 October 2025

Abstract

Sialic acids are a diverse family of acidic sugars typically found at the terminal positions of glycan chains, mediating key physiological and pathological processes across animals - particularly vertebrates - including cell signaling and host-pathogen interactions. The distribution of sialic acids in lower animals such as mollusks, however, remains largely unresolved. Here, we report the discovery of unconjugated 2-keto-3-deoxy-D-glycero-D-galacto-nononic acid (KDN), a deaminated analogue of *N*-acetylneuraminic acid, in the muscle tissue of Pacific oysters (*Magallana gigas*). Using UPLC-ESI-MS/MS fingerprinting, we identified naturally occurring free KDN at a concentration of 1.2 ± 0.1 nmol/100 mg of oyster muscle tissue. To investigate the biosynthetic pathway, four candidate genes were identified in the *M. gigas* genome, and the corresponding recombinant proteins were expressed and characterized. Enzymatic assays revealed that one putative sialic acid aldolase (MgNPL) specifically catalyzes the cleavage of KDN into mannose and pyruvate. To our knowledge, this represents the first molecular evidence of KDN metabolism in mollusks and highlights both the unexpected conservation of substrate-specific aldolase activity and distinct sialic acid utilization mechanisms compared to vertebrates.

Keywords Nonulosonic acids · Sialic acid aldolase · Invertebrate glycobiology · KDN analogues · Mollusk biochemistry

Introduction

Sialic acids are a diverse family of nine-carbon acidic monosaccharides typically found at the terminal positions of glycan chains on the surfaces of eukaryotic cells, where they play pivotal roles in cell communication, development, and host-pathogen interactions [1]. The most common sialic acid variants include *N*-acetylneuraminic acid (Neu5Ac), which is prevalent across vertebrates, and *N*-glycolylneuraminic acid (Neu5Gc), mainly found in non-human mammals, which are differentiated primarily by substitutions at the C5 position. Less widely distributed but notable is 2-keto-3-deoxy-D-glycero-D-galacto-nononic acid (KDN), a deaminated analogue of Neu5Ac, which can occur either as free molecules or as components of complex glycan structures *via* various linkages [2–4]. Notably, aberrant expression or metabolism of sialic acids - particularly KDN - has been associated with various pathological processes, including autoimmunity, inflammation, metabolic disorders, and malignancies such as ovarian, breast, lung, and pancreatic cancers. The rare occurrence of KDN in healthy

✉ Li Liu
lichen.liu@njau.edu.cn

✉ Josef Voglmeir
josef.voglmeir@njau.edu.cn

[1] Glycomics and Glycan Bioengineering Research Center (GGBRC), College of Food Science and Technology, Nanjing Agricultural University, 1 Weigang, Nanjing 210095, China

[2] Department of Biotechnology, Faculty of Applied Sciences, Delft University of Technology, Van der Maasweg 9, Delft 2629 HZ, The Netherlands

[3] Institute of Biocomputation and Physics of Complex Systems (BIFI), University of Zaragoza, Calle Mariano Esquillor, Edificio I+D, Zaragoza 50018, Spain

[4] School of Chemistry, University of Bristol, Cantock's Close, Bristol BS8 1TS, UK

Published online: 19 December 2025

human tissues and its prominence in tumor contexts have spurred interest in its utility as a tumor-associated carbohydrate biomarker for early cancer detection [5–11].

The biosynthesis of sialic acids originates in the cytosol from UDP-N-acetylglucosamine, proceeding through a cascade of enzymes such as UDP-GlcNAc 2-epimerase/ManNAc kinase (GNE), sialic acid phosphatase (NANP), and culminating in activation by CMP-sialic acid synthetase (CMAS) for glycan integration in the Golgi apparatus (Fig. 1) [12, 13]. Sialic acid catabolism is tightly regulated by sialic acid aldolases (NPLs), which cleave sialic acids into underlying monosaccharides and pyruvate, and dysregulation of this pathway can lead to skeletal and cardiac myopathies [14, 15].

KDN was first identified in rainbow trout eggs and has since been detected in other lower vertebrates, certain bacterial species, and to a lesser extent in mammals; however, its occurrence and biological significance in invertebrates (particularly in mollusks) remain largely unexplored [16–20]. Previous studies have reported the presence of sialic acid-binding lectins in oysters [21–23], suggesting a possible role for sialic acids in the immune functions of these organisms. Nevertheless, direct evidence supporting the existence, diversity, and metabolism of sialic acids such as KDN in oysters is lacking, and the specific biosynthetic pathways involved have yet to be elucidated. This knowledge gap is compounded by technical challenges: the inherently low abundance and structural heterogeneity of sialic acids in molluscan tissues have historically hindered their detection and comprehensive characterization.

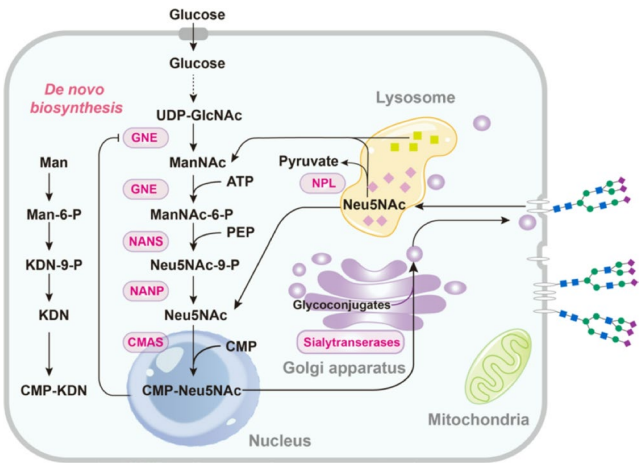

Fig. 1 Schematic representation of the de novo biosynthesis pathway of sialic acids. A sequence of enzymatic reactions mediates the biosynthesis, activation, and conjugation of sialic acids. Key enzymes include UDP-GlcNAc 2-epimerase/ManNAc kinase (GNE), sialic acid synthase (NANS), sialic acid phosphatase (NANP), and CMP-sialic acid synthase (CMAS), which converts sialic acids into CMP-sialic acid. This activated form is subsequently transported to the Golgi apparatus, where sialyltransferases catalyze the sialylation of glycoconjugates, resulting in the formation of sialoglycoconjugates. Sialic acids released from lysosomes can re-enter the cytosol to undergo another sialylation cycle in the Golgi apparatus. Additionally, sialic acids may be reversibly converted to pyruvate and ManNAc by sialic acid lyase (NPL)

Notably, comprehensive glycomic analyses of *Crassostrea species* have revealed complex anionic modifications (phosphate and sulfate) on hemocyanins and mucosal glycoproteins, yet no definitive evidence of sialylated N- or O-glycans exists to date [21, 24]. This absence contrasts with reported sialic acid-binding lectins in oysters, suggesting potential evolutionary divergence in sialoglycan recognition systems [22, 23].

Recent analytical advances - particularly the advent of highly sensitive techniques such as liquid chromatography coupled with tandem mass spectrometry (LC-MS/MS) - now allow for the precise detection and structural annotation of sialic acids, even within complex biological samples [7, 25, 26]. In addition, the recent identification of a sialic acid aldolase homolog in snails prompted us to investigate the potential occurrence of nonulosonic acids (NPLs) in oysters [27]. Here, we combine quantitative profiling of KDN in oyster tissue lysates with genomic analyses to uncover the molecular basis of sialic acid biosynthesis in this organism. This approach not only clarifies the presence and metabolism of KDN in oysters but also provides a fresh impulse on the evolutionary and biological significance of sialic acids in invertebrate systems.

Experimental procedures

Plasmids, materials and chemicals

The putative *N*-acetylneuraminate pyruvate lyase (NPL) gene sequence was identified by mining the *Magallana gigas* genome for homologs of the human NPL variant. The top hit (NCBI gene sequence LOC105330010, Figure S1) was then synthesized by GenScript Biotechnology Co., Ltd. (Nanjing, China). Oligonucleotide primers for site-directed mutagenesis of the MgNPL mutant variant were designed and obtained from Tsingke Biotech Co., Ltd. (Beijing, China). Fresh raw oysters were sourced from Shandong Lighthouse Jellyfish Marine Technology Co., Ltd. (Weihai, China). KDN and its analogues (5-*epi*-KDN and 5,7-di-*epi*-KDN) were synthesized following our established procedures [28]. Thin layer chromatography (TLC) plates (Type 60 F_{254}), anion exchange resin, acetic acid, and ammonium acetate were purchased from General-reagent Co., Ltd. (Nanjing, China). Acetonitrile (ACN) and methanol (MeOH) used for HPLC-ESI-MS and tandem MS/MS analyses were supplied by Merck Ltd. (Darmstadt, Germany). All other reagents and solvents were of the highest analytical grade and obtained from local commercial suppliers.

Mutagenesis, expression and purification of MgNPL

The lysine-to-alanine mutant variant (K174A) was generated using the QuickChange site-directed mutagenesis protocol (Stratagene), with the MgNPL plasmid serving as the DNA template (see Figure S1). The forward primer sequence was 5'-GAACCTGATCGGTCTGGCGTTCGCT TCTAAAGACC-3', and the reverse primer sequence was 5'-GGTCTTTAGAAGCGAACGCCAGACCGATCAGG TTC-3'. Following mutagenesis, both wild-type MgNPL and the K174A mutant plasmids were transformed into *E. coli* BL21 (DE3) competent cells ($LacZ^-$) *via* heat-shock transformation. The recombinant strains harboring pET30a-MgNPL (wild-type and mutant) were first cultured overnight at 37 °C, 180 rpm in 5 mL LB medium containing 50 μg/mL kanamycin. The overnight cultures were then used to inoculate 400 mL of sterilized LB medium (with 50 μg/mL kanamycin), which was incubated at 37 °C until the optical density at 600 nm (OD_{600}) reached 0.7. Protein expression was induced by adding 400 μL of 1 M IPTG and incubating at 18 °C, 180 rpm for 20 h. Cells were harvested by centrifugation at 4,000 rpm for 10 min at 4 °C. The cell pellets were resuspended in 10 mL lysis buffer (50 mM Tris-HCl, 100 mM NaCl, 1% Triton X-100) and lysed by sonication in the presence of 1 mM PMSF, using 20 min cycles (10 sec on/10 sec off). The lysates were centrifuged at 12,000 rpm for 20 min at 4 °C to remove debris. The resulting supernatant was applied to a Ni-NTA agarose column (2 mL bed volume; Qiagen, Shanghai, China). The column was washed with buffer containing 50 mM Tris-HCl and 50 mM NaCl, and bound proteins were eluted with buffer containing 50 mM Tris-HCl, 50 mM NaCl, and 200 mM imidazole (pH 8.0). Purified proteins were stored in 20% (v/v) glycerol at −80 °C for further use. The expression and purity of wild-type and mutant MgNPL were confirmed by SDS-PAGE, with bands visualized using Coomassie Brilliant Blue G-250 staining.

Enzymatic activity assay

Recombinant *Dyadobacter fermentas N*-acetylneuraminic pyruvate lyase (DfNPL) was used to synthesize KDN, 5-*epi*-KDN, and 5,7-di-*epi*-KDN, which were subsequently purified by silica gel chromatography according to a previously published protocol [29]. For sialic acid cleavage assays, reaction mixtures (50 μL total volume) containing 8 mM sialic acid, 100 mM Tris-HCl (pH 7.5), and recombinant enzyme (~ 20 μg) were incubated at 37 °C for 12 h. After incubation, the reactions were terminated by heating at 95 °C for 10 min, followed by centrifugation at 12,000 rpm at 4 °C for 10 min. For initial assessment of enzymatic activity, 1 μL aliquots of each supernatant were applied to thin-layer chromatography (TLC) plates. The plates were developed using n-butanol/acetic acid/water (5:3:2, v/v/v) as the mobile phase and visualized with DPA staining solution (prepared by dissolving 5.91 mmol diphenylamine and 10.75 mmol aniline in 50 mL acetone and 5 mL phosphoric acid).

For sialic acid synthesis assays, reaction mixtures (50 μL) containing 200 mM aldose (mannose, glucose, or galactose), 1 M sodium pyruvate, 50 mM Tris-HCl (pH 7.5), and recombinant enzyme (~20 μg) were incubated at 37 °C for 12 h. Reactions were halted by heating at 95 °C for 10 min and subsequently centrifuged at 12,000 rpm for 10 min. A 20 μL aliquot of the supernatant was mixed with 50 μL o-phenylenediamine solution (10 mg/mL o-phenylenediamine dissolved in 200 mM sodium bisulfite) and incubated at 80 °C for 45 min for derivatization. The mixture was then centrifuged at 12,000 rpm for 5 min, and the resulting supernatant was subjected to HPLC-FLD-MS analysis.

Sialic acid extraction from oyster muscle tissue

Fresh oysters were thoroughly washed and shucked. The oyster muscle tissue was cut into small pieces and freeze-dried under vacuum to remove moisture. Sialic acids were then extracted from the freeze-dried oyster tissue according to previously established procedures with minor modifications [30, 31]. Briefly, 100 mg of freeze-dried tissue was homogenized in 1.2 mL of double-distilled water (ddH_2O) using a 2 mL glassware grinder. The homogenate was transferred to a 2 mL Eppendorf tube and centrifuged at 4 °C, 12,000 g for 15 min. One milliliter of the resulting supernatant was loaded onto an anion exchange resin column (200 mg Dowex 1 × 8, 100–200 mesh, Cl^- form), pre-equilibrated sequentially with 2 mL of 2 M acetic acid and 2 mL of ddH_2O (three times). After loading the sample, 2.4 mL of ddH_2O was added, and sialic acids were eluted from the resin with 1.2 mL of 50 mM ammonium acetate. Eluted fractions were pooled and concentrated by centrifugal evaporation under vacuum.

For the sialic acid derivatization, 20 μL of DAPMI reagent [31] (10 mg/mL in 0.2 M sodium bisulfite) was added to the dried samples. The mixture was incubated at 80 °C for 45 min, followed by centrifugation at 4 °C, 12,000 rpm for 15 min. The resulting supernatants were subjected to UPLC-ESI-MS/MS analysis (Scheme S1, Figure S2).

HPLC-FLD-MS analysis

The enzymatic activity assay was performed using a Nexera HPLC-FLD-MS system (Shimadzu Corporation, Kyoto, Japan), comprising an LC-30AD pump with a low-pressure gradient mixing unit, a SIL-30AC autosampler, and an

RF-20Axs fluorescence detector. Analytes (20 µL) were injected onto a reversed-phase HPLC column (Cosmosil 5C18 MS-II, 4.6 × 250 mm; Nacalai Inc., Japan) and separated at a constant flow rate of 1.0 mL/min. Fluorescence detection was performed with excitation/emission wavelengths of 373/448 nm. The elution solvents consisted of solvent A (100% H_2O), solvent B (100% acetonitrile), and solvent C (100% methanol). Separation was achieved using the following linear gradient: 5–12% solvent B and C from 0 to 10 min; 12–40% B and C from 10 to 12 min, maintained at 40% for 4 min; then, solvent B and C were reduced to 5% over 1 min and held under this condition for 5 min to re-equilibrate the column.

LC-MS/MS analysis of sialic acids

Qualitative and quantitative analyses of sialic acids were conducted using a Shimadzu LCMS-8040 triple quadrupole tandem mass spectrometer. A 5 µL aliquot of analyte derivatized with DAPMI was injected onto an Acquity BEH Amide column (2.1 × 150 mm, 1.7 µm; Waters, Ireland) maintained at 60 °C. The mobile phases were solvent A (50 mM ammonium formate, pH 4.5) and solvent B (acetonitrile), delivered at a flow rate of 0.4 mL/min. Gradient elution was performed as follows: 88% B for 0–1.5 min; 88% to 70% B from 1.5 to 35 min; 70% to 0% B from 35 to 35.5 min (held for 0.5 min); and re-equilibration at 88% B from 36 to 44.5 min. Detection was carried out with an RF-20Axs fluorescence detector (λ_{ex} = 356 nm, λ_{em} = 412 nm) and the LCMS-8040 equipped with an ESI-ToF detector operating in positive ion mode. The mass spectrometer was operated with a detector voltage of 1.5 kV, interface temperature of 350 °C, desolvation tube temperature of 250 °C, and heating module at 200 °C. Nebulizer and drying gas flow rates were set at 3 L/min and 15 L/min, respectively. Data were analyzed using Shimadzu Lab Solutions software (version 5.91).

UPLC-ESI-HRMS/MS fragment ion profiling

HRMS/MS analysis of DMB-NulOs was performed as described recently [32, 33]. Briefly, DMB-derivatized extracts were analyzed using an Acuity UPLC system (Waters, UK) equipped with a C18 1.7 µm BEH separation column coupled to a QE Focus Orbitrap mass spectrometer (Thermo Scientific, Germany). Solvent A consisted of 97% H_2O and 3% acetonitrile, and solvent B consisted of 97% acetonitrile and 3% H_2O (both containing 0.1% formic acid). The Orbitrap was operated in ESI + mode alternating full scans and small mass window fragmentation scans for untargeted screening, or alternatively, PRM analysis targeting the m/z of DMB-KDN (385.1242) was performed. Interpretation of fragment ion peaks of detected NulOs was performed according to Kleikamp et al. [33], Finally, the fragment-ion profiles of Oyster KDN was statistically compared to synthetic KDN standards using Xcalibur Software (Thermo Scientific) and Python within the Spyder IDE.

Statistical analysis

Origin 2024b software (version 10.1.5.132) was used for statistical analysis of sialic acid quantification and data processing of MS/MS fragment profiles. Multivariate statistical analysis, including principal component analysis (PCA) and hierarchical cluster analysis (HCA), was carried out using R software (https://www.r-project.org) coupled with RStudio visual interface (version 1.1.463). For hierarchical cluster analysis (HCA), the between-groups linkage method was used for clustering, and Euclidean distance was selected as the distance measurement method.

Results and discussion

UPLC-ESI-MS/MS analysis of free Sialic acids in oyster muscle tissue

To assess the endogenous sialic acid profile in Pacific oyster muscle tissue, UPLC-ESI-MS/MS was performed following DAPMI derivatization. The analysis demonstrated that neither N-acetylneuraminic acid (Neu5Ac) nor N-glycolylneuraminic acid (Neu5Gc), two sialic acid forms commonly found in vertebrates, were detected in the oyster lysates (Fig. 2A). However, a mass signal consistent with the deaminated sialic acid analogue 2-keto-3-deoxy-D-glycero-D-galacto-nononic acid (KDN) was observed at a concentration of 1.2 ± 0.1 nmol per 100 mg of oyster muscle tissue (Fig. 2B).

UPLC-ESI tandem MS/MS analysis of oyster-derived KDN and analogues

To validate the distinctive KDN-related fragmentation patterns observed in the oyster muscle lysates, we performed detailed UPLC-ESI-MS/MS analysis using DMB derivatization, comparing fragmentation fingerprints with standard KDN isomers. Product ion MS/MS spectra from DMB-labeled sialic acids are illustrated in Fig. 3A. The oyster muscle tissue samples exhibited several prominent fragment ions (notably m/z 205, 217, 229, 271, and 313), closely matching those produced by standard KDN isomers (KDN 1b, 5-*epi*-KDN 1c, and 5,7-di-*epi*-KDN 1 d). The proposed fragmentation pathway for DMB-KDN (Scheme S2, Fig. 3B) aligns with established sialic acid

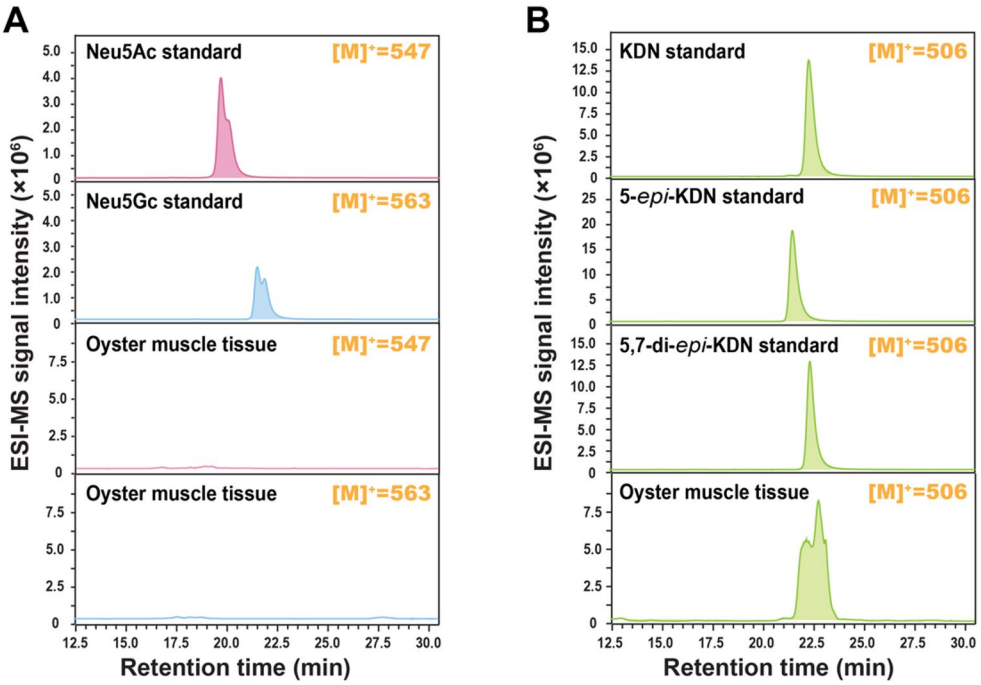

Fig. 2 UPLC-ESI-MS determination of sialic acids in oyster muscle tissue after DAPMI fluorescent tag derivatization (positive single ion mode), and composition analysis of **(A)** Neu5Ac, Neu5Gc, and **(B)** KDN with its analogues in oyster muscle tissues

fragmentation behavior, revealing reproducible intermediate fragments (M1-M6) generated stepwise from the precursor (M7), with the m/z 205 ion (M1) presenting the greatest relative intensity. These diagnostic ion fragments are critical for robustly assigning sialic acid structural features within oyster muscle tissue.

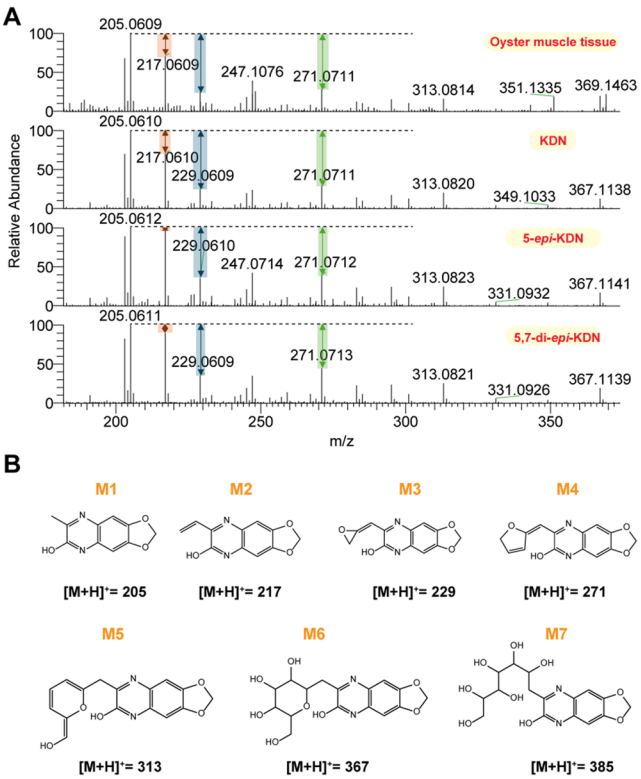

Fig. 3 **(A)** UPLC-ESI tandem MS/MS fragment spectra of sialic acids in oyster tissues following DMB derivatization. **(B)** Proposed structures of key fragment ions (M1-M6) derived from the precursor DMB-KDN (M7)

In total, 50, 51, 52, and 51 MS/MS fragments were identified in oyster tissue, KDN 1b, 5-*epi*-KDN 1c, and 5,7-di-*epi*-KDN 1 d, respectively (see Supporting Information, Tables S1–S4). Fragment count alone was insufficient to fully distinguish oyster KDN from its analogues. Therefore, hierarchical clustering analysis (HCA) based on the fragmentation profiles of key representative ions (CM1–CM19) was undertaken, effectively separating oyster and KDN 1b from 1c and 1 d (Fig. 4A). CM1 (m/z 203), CM3 (m/z 205), and CM5 (m/z 217) substantially contributed to discrimination, alongside additional marker ions such as CM7 (m/z 229), CM12 (m/z 247), and CM15 (m/z 271), with relative abundance accounting for 21.7–43.6% (Table S5).

The separation of oyster KDN from 5-*epi*-KDN and 5,7-di-*epi*-KDN in HCA led us to investigate the underlying stereochemical implications. We initially hypothesized that 5-*epi*-KDN might be present, as its formation from glucose (rather than mannose) could suggest evolutionary links to glucose metabolism. To further resolve differences between sample types, principal component analysis (PCA) was performed, yielding a cumulative contribution of 99.4% for PC1 and PC2 (85.5% for PC1, 13.9% for PC2; Fig. 4B). Oyster tissue and KDN 1b groups clustered closely in both principal components, in contrast to the distinct separation of 1c and 1 d, consistent with HCA findings. Although isomers 1c and 1 d overlapped in PC1, they could be differentiated along PC2. Dot product analysis of key fragment spectra (M1–M4) confirmed very high similarity between

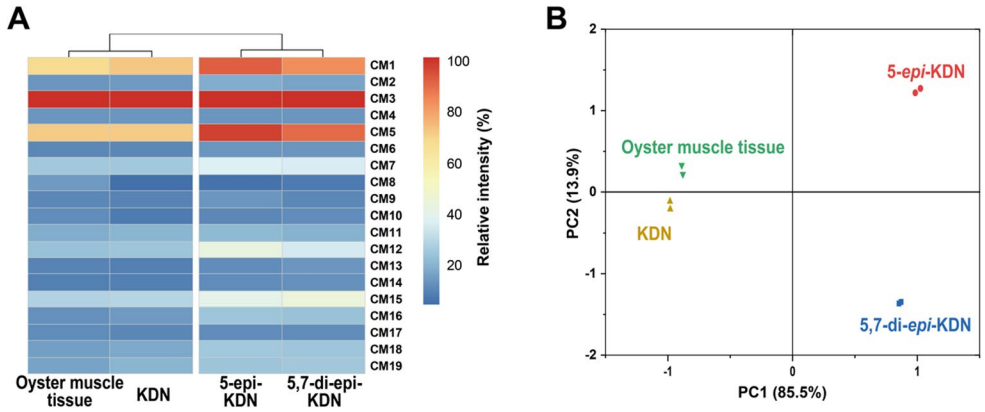

Fig. 4 Comparison of UPLC-ESI MS/MS fragmentation fingerprints among oyster muscle tissue, KDN, 5-epi-KDN, and 5,7-di-epi-KDN. **(A)** Heatmap displaying the intensity distribution of common product ions (m/z 200–385 Da) across sample groups, analyzed by hierarchical clustering analysis (HCA). Color gradients from blue to red indicate the range of relative intensity (0–100%). **(B)** Principal component analysis (PCA) score plot differentiating sample species based on the relative abundance of key fragment ions (M1–M4) as multivariate variables. The diagnostic fragment ions sets CM1-CM19 are listed in Table S5

oyster and 1b (DP = 1.0), with slightly lower but still strong similarities observed for oyster with 1c (DP = 0.9872) and 1 d (DP = 0.9888), substantiating the predominance of KDN-like features in oyster sialic acid profiles (Figure S3).

These results collectively demonstrate that the fragmentation patterns of sialic acids from oyster tissue closely resemble those of standard KDN isomers, particularly KDN 1b, supporting the conclusion that KDN is the main type of sialic acid present in oyster muscle tissue.

Molecular basis of Sialic acid presence in oysters

To investigate the underlying molecular basis of the sialic acid metabolism in Pacific oysters, a BLAST search of the *M. gigas* cDNA library identified a putative ortholog of the *N*-acetylneuraminate pyruvate lyase (NPL) gene referred to as MgNPL. To probe the functional importance of key active site residues, site-directed mutagenesis was performed on lysine 174, which is essential for Schiff base intermediate formation in NPL catalysis; this residue was replaced with alanine. Both wild-type MgNPL and its K174A mutant variant were recombinantly expressed in *E. coli* BL21 (DE3). Efficient soluble expression and subsequent purification by nickel-chelation affinity chromatography yielded approximately 5 mg of each enzyme from 400 mL of fermentation broth, with protein integrity retained after storage at −80 °C for over six months, as confirmed by SDS-PAGE (Fig. 5A, Figure S4).

While our study conclusively demonstrates free KDN presence in oyster muscle tissue, the experimental design focused on free sialic acid detection through ion exchange chromatography and DAPMI derivatization, which inherently limits conjugate identification. This methodological framework suggests either that KDN exists exclusively in free form within muscle tissue, or that KDNase-mediated cleavage of conjugates occurs prior to detection. The latter hypothesis aligns with previous reports of KDNase activity in *Crassostrea virginica* hepatopancreas extracts, suggesting potential enzymatic activity preservation across oyster tissues [34]. The selective analysis of oyster muscle tissue reduced the likelihood of gut microbiota-derived KDN.

While this study provides novel insights into KDN metabolism in *M. gigas*, several technical constraints of the current study should also be mentioned. As we only used oyster muscle tissue for our analysis, a detailed compartmentalization of KDN or conjugation patterns in distinct anatomical regions could not be determined. In addition, the protocol used in this work only focused on the isolation of free KDN and not glycosidically-bound KDN forms. Furthermore, while muscle tissue analysis reduces likelihood of gut microbiota-derived KDN, we did not perform systematic microbiota depletion across all sampled tissues, leaving open the possibility of marine biofilm contributions to free KDN pools - particularly in gill and mantle samples that interface directly with environmental microbes. These limitations highlight the need for future studies employing tissue-specific microdissection, KDN-enrichment strategies for conjugate detection, and controlled aquaculture conditions with microbial profiling to fully resolve endogenous versus exogenous KDN sources.

The apparent paradox between lectin presence and glycan absence raises some interesting questions about the biological role of KDN in oysters. The oyster's sialic acid-binding lectins [22, 23] likely recognize microbial sialic acids as part of innate immunity, analogous to vertebrate siglecs. This lectin specificity for KDN-containing structures may be therefore used for pathogen surveillance through KDN-mediated molecular mimicry detection or endogenous

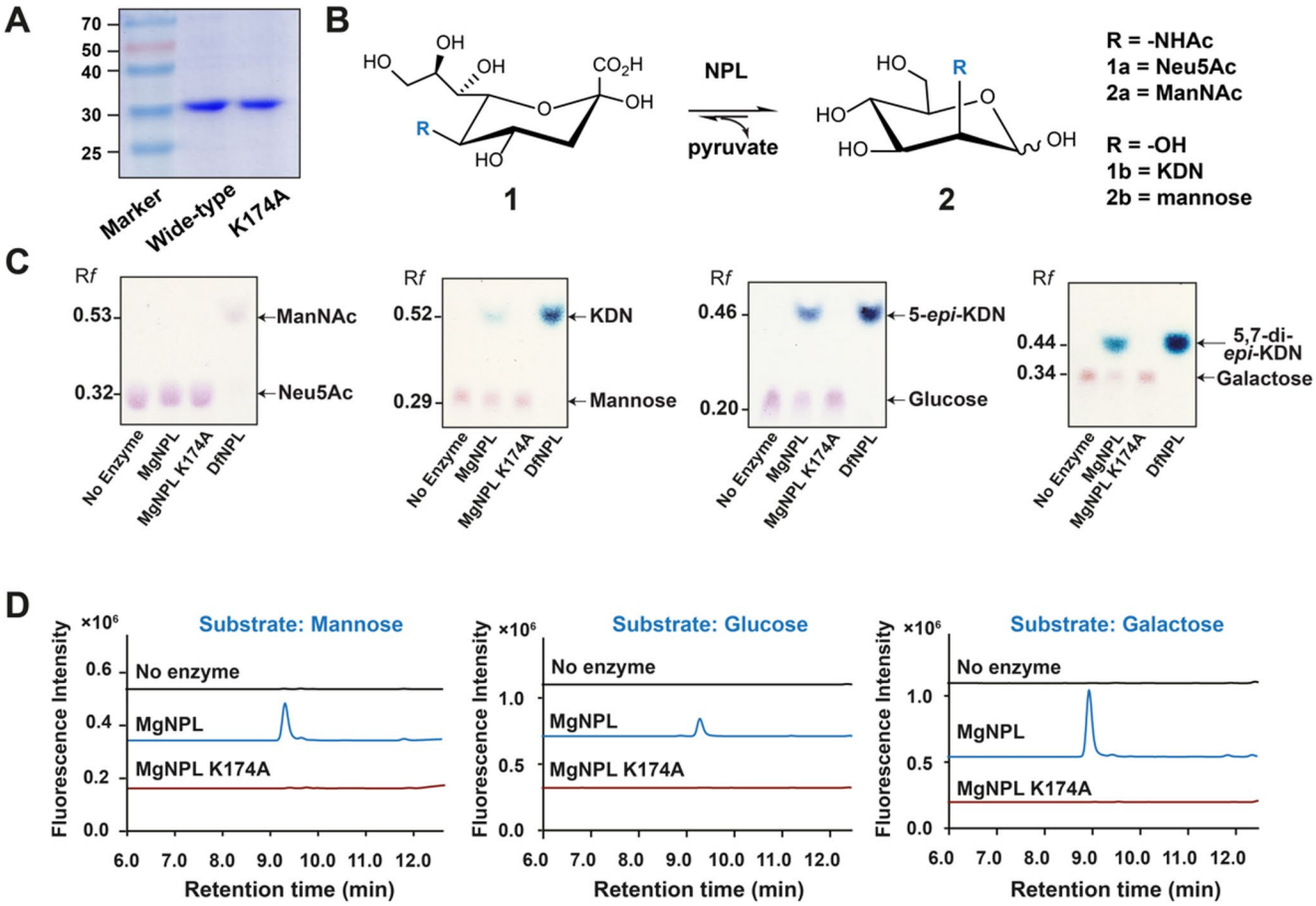

Fig. 5 **(A)** SDS-PAGE analysis showing purified wild-type MgNPL and the K174A mutant after Ni-NTA affinity chromatography. **(B)** Schematic overview of *N*-acetylneuraminate pyruvate lyase (NPL)-catalyzed reverse synthesis of sialic acids (Sias 1) from the corresponding aldoses (2) and pyruvate. **(C)** Thin-layer chromatography (TLC) analysis of enzyme activity toward different sialic acids (Neu5Ac 1a, KDN 1b, 5-*epi*-KDN 1c, and 5,7-di-*epi*-KDN 1 d). **(D)** HPLC-fluorescence detection (Ex/Em = 373 nm/448 nm) of enzymatic synthesis of KDN and its analogues using mannose (2b), glucose (2c), or galactose (2d) with pyruvate as substrates

signaling through free KDN as a damage-associated molecular pattern. The strict KDN specificity of MgNPL may therefore complement these lectins, potentially forming a coordinated system for KDN recycling during immune challenges.

Enzymatic activity

The catalytic properties of MgNPL were initially characterized by its ability to cleave sialic acid substrates including Neu5Ac (1a), KDN (1b), 5-*epi*-KDN (1c), and 5,7-di-*epi*-KDN (1d) into pyruvate and their respective aldoses - ManNAc (2a), mannose (2b), glucose (2c), and galactose (2d) - as analyzed by TLC. Strikingly, MgNPL exhibited activity toward KDN and its analogues (1b–d), but no detectable cleavage of Neu5Ac (1a); the K174A mutant displayed no activity toward any substrate, confirming the essential role of lysine 174 (Table S6, Fig. 5B–C). These findings were corroborated by UPLC-fluorescence detection (FLD)-based assays after 1,2-diaminobenzene (OPD) derivatization (Figure S5).

Further HPLC-FLD analysis demonstrated that MgNPL efficiently synthesized KDN and its structural analogues (1b–d) from pyruvate and the appropriate aldoses, but did not generate Neu5Ac from ManNAc and pyruvate (1a) under the tested conditions (Fig. 5D, Figure S6).

The observed catalytic specificity of MgNPL for KDNs mirrors the behavior previously reported for a freshwater snail sialic acid aldolase (sNPL), which also displays negligible activity toward Neu5Ac, suggesting a possible divergence in NPL substrate usage among invertebrates compared to vertebrates [27, 35]. Additionally, parallels with a KDN-specific aldolase from *Sphingobacterium sp.* - which exclusively degrades KDN but not Neu5Ac or Neu5Gc [36] - further support the hypothesis that mollusks like oysters may utilize a KDN-centric metabolic system, possibly involving specialized sialidases and NPLs adapted for efficient turnover of KDN-type sialic acids.

Conclusion

This study provides the first molecular and biochemical evidence for the presence and metabolism of sialic acids in the Pacific oyster (*Magallana gigas*). Using UPLC-ESI-MS/MS analysis, we detected only unconjugated KDN and its structural analogues in oyster muscle tissue, with no evidence for more common vertebrate sialic acids such as Neu5Ac or Neu5Gc. Functional characterization of a recombinant oyster sialic acid aldolase (MgNPL) revealed that it specifically catalyzes the reversible formation and cleavage of KDN and its analogues, but does not act on Neu5Ac, confirming its substrate specificity and suggesting a unique KDN-centered metabolic pathway in oysters. These findings not only expand our understanding of sialic acid diversity and metabolism in invertebrates but also highlight oysters as a valuable model for studying the evolutionary adaptation of sialic acid biosynthesis and catabolism beyond vertebrate systems. Our findings provide biochemical evidence for KDN cycling in *M. gigas*, though the physiological role remains unclear given current limitations in comprehensively understanding all aspects of mollusk glycobiology. The strict KDN specificity of MgNPL contrasts with the broader substrate tolerace of vertebrate promiscuous aldolases, suggesting functional adaptation to ancestral deaminated sialic acid metabolism. We hope anticipate that this work will help to explore further biological roles of KDN in mollusks and set the stage for investigating the broader evolutionary and functional landscape of sialic acids in non-vertebrate species.

Contributions

Zi-Xuan Hu: Writing – original draft, Visualization, Formal analysis, Data curation. Jia-Yu Zhang: Formal analysis, Data curation. Jitske van Ede: Resources, Visualization, Formal analysis, Data curation. Yu-Quan Li: Data curation. Yao-Yao Zhang: Formal analysis, Data curation. Mattia Ghirardello: Formal analysis, Data curation. M. Carmen Galan: Resources, Conceptualization, Supervision. Martin Pabst: Writing – review & editing, Visualization, Supervision, Resources. Li Liu: Writing – review & editing, Supervision, Conceptualization. Josef Voglmeir: Writing – original draft, review & editing, Visualization, Supervision, Resources, Data curation, Conceptualization.

Abbreviations

UDP-GlcNAc	UDP-*N*-acetylglucosamine
ManNAc	UDP-GlcNAc 2-epimerase/*N*-acetylmannosamine kinase
GNE	
NANS	*N*-acetylneuraminic acid synthase
NANP	*N*-acetylneuraminic acid phosphatase
CMAS	*N*-acylneuraminate cytidylyltransferase
CMP-Neu5Ac	Cytidine-5-monophosphoneuraminic acid
ManNAc	*N*-acetylmannosamine
GlcNAc	*N*-acetylglucosamine
NPL	Neuraminic acid pyruvate-lyase
PEP	Phosphoenolpyruvate
Man-6-P	Mannose 6-phosphate
UPLC-ESI-MS	Ultra high performance liquid chromatography- electrospray ionization-mass spectrometry
NulOs	Nonulosonic acids
PCA	Principal component analysis
HCA	Hierarchical cluster analysis

Supplementary Information The online version contains supplementary material available at https://doi.org/10.1007/s10719-025-10202-0.

Acknowledgements This study was funded by the National Natural Science Foundation of China (NSFC) 31871793, 31871754, and W2432055 (to J.V. and L.L.), and MCG thanks EPSRC GCRFE (Grant Nos. P/T020288/1 and EP/S026215/1 and ERC-COG: 648239. M.G. thanks the Scientific Foundation of the Spanish Association Against Cancer (INVES246008GHIR) for supporting this work. This study was partly performed on the platform of the Department of Biotechnology, Faculty of Applied Sciences, Delft University of Technology, Van der Maasweg 9, 2629 HZ Delft (The Netherlands).

Author contributions Zi-Xuan Hu: Writing – original draft, Visualization, Formal analysis, Data curation. Jia-Yu Zhang: Formal analysis, Data curation. Jitske van Ede: Resources, Visualization, Formal analysis, Data curation. Yu-Quan Li: Data curation. Yao-Yao Zhang: Formal analysis, Data curation. Mattia Ghirardello: Formal analysis, Data curation. M. Carmen Galan: Resources, Conceptualization, Supervision. Martin Pabst: Writing – review & editing, Visualization, Supervision, Resources. Li Liu: Writing – review & editing, Supervision, Conceptualization. Josef Voglmeir: Writing – original draft, review & editing, Visualization, Supervision, Resources, Data curation, Conceptualization.

Data availability No datasets were generated or analysed during the current study.

Declarations

Competing interests The authors declare no competing interests.

References

1. Varki, A., Schauer, R.: Sialic acids. In: Varki, A., Cummings, R.D., Esko, J.D., Freeze, H.H., Stanley, P., Bertozzi, C.R., Hart, G.W., Etzler, M.E. (eds.) Essentials of Glycobiology. Cold Spring Harbor (NY (2009)
2. Pearce, O.M.T., LäUBLI, H.: Sialic acids in cancer biology and immunity. Glycobiology. **26**, 111–128 (2015)
3. Samraj, A., Läubli, H., Varki, N., Varki, A.: Involvement of a Non-Human Sialic Acid in Human Cancer. Front Oncol **4**, 33 (2014)

4. Sadako, I., Kitajima, K.: KDN (deaminated neuraminic acid): Dreamful past and exciting future of the newest member of the Sialic acid family. Glycoconj. J. **23**, 277–290 (2006)
5. Guerrero-Flores, G.N., Pacheco, F.J., Boskovic, D.S., Pacheco, S.O.S., Zhang, G., Fraser, G.E., Miles, F.L.: Sialic acids Neu5Ac and KDN in adipose tissue samples from individuals following habitual vegetarian or non-vegetarian dietary patterns. Sci Rep **13**, 12593 (2023)
6. Sethi, M.K., Hancock, W.S., Fanayan, S.: Identifying N-Glycan Biomarkers in Colorectal Cancer by Mass Spectrometry. Acc Chem Res **49**, 2099–2106 (2016)
7. Wang, F., Xie, B., Wang, B., Troy, F.A.: LC–MS/MS glycomic analyses of free and conjugated forms of the Sialic acids, Neu5Ac, Neu5Gc and KDN in human throat cancers. Glycobiology. **25**, 1362–1374 (2015)
8. Yabu, M., Korekane, H., Hatano, K., Kaneda, Y., Nonomura, N., Sato, C., Kitajima, K., Miyamoto, Y.: Occurrence of free deaminoneuraminic acid (KDN)-containing complex-type N-glycans in human prostate cancers. Glycobiology. **23**, 634–642 (2013)
9. Ghosh, M., Hazarika, P., Dhanya, S.J., Pooja, D., Kulhari, H.: Exploration of sialic acid receptors as a potential target for cancer treatment: A comprehensive review. Int J Biol Macromol **257**, 128415 (2024)
10. Go, S., Sato, C., Yin, J., Kannagi, R., Kitajima, K.: Hypoxia-enhanced expression of free deaminoneuraminic acid in human cancer cells. Biochem. Biophys. Res. Commun. **357**, 537–542 (2007)
11. Inoue, S., Kitajima, K., Sato, C., Go, S.: Human KDN (Deaminated neuraminic Acid) and its elevated expression in cancer cells: Mechanism and significance. In: Wu, A.M. (ed.) The Molecular Immunology of Complex Carbohydrates-3, 2011//, pp. 669–678. Springer, Boston, MA (2011)
12. Zhou, X., Yang, G., Guan, F.: Biological functions and analytical strategies of Sialic acids in tumor. Cells. **9**, 1–18 (2020)
13. Zhu, W., Zhou, Y., Guo, L., Feng, S.: Biological function of Sialic acid and sialylation in human health and disease. Cell. Death Discov. **10**, 415 (2024)
14. Wen, X.-Y., Tarailo-Graovac, M., Brand-Arzamendi, K., Willems, A., Rakic, B., Huijben, K., da Silva, A., Pan, X., El-Rass, S., Ng, R., Selby, K., Philip, A.M., Yun, J., Ye, X.C., Ross, C.J., Lehman, A.M., Zijlstra, F., Abu Bakar, N., DRöGEMöLLER, B., Moreland, J., Wasserman, W.W., Vallance, H., van Scherpenzeel, M., Karbassi, F., Hoskings, M., Engelke, U., de Brouwer, A., Wevers, R.A., Pshezhetsky, A.V., van Karnebeek, C.D.M., Lefeber, D.J.: Sialic acid catabolism by N-acetylneuraminate pyruvate lyase is essential for muscle function. JCI Insight **3**, e122373 (2018)
15. da Silva, A., Dort, J., Orfi, Z., Pan, X., Huang, S., Kho, I., Heckel, E., Muscarnera, G., van Vliet, P.P., Sturiale, L., Messina, A., Romeo, D.A., van Karnebeek, C.D.M.W.E.N.X.-Y., Hinek, A., Molina, T., Andelfinger, G., Ellezam, B., Yamanaka, Y., Olivos, H.J., Morales, C.R., Joyal, J.-S., Lefeber, D.J., Garozzo, D., Dumont, N.A., Pshezhetsky, A.V.: N-acetylneuraminate pyruvate lyase controls sialylation of muscle glycoproteins essential for muscle regeneration and function. Sci Adv. **9**, eade6308 (2023)
16. Nadano, D., Iwasaki, M., Endo, S., Kitajima, K., Inoue, S., Inoue, Y.: A naturally occurring deaminated neuraminic acid, 3-deoxy-D-glycero-D-galacto-nonulosonic acid (KDN). Its unique occurrence at the nonreducing ends of oligosialyl chains in polysialoglycoprotein of rainbow trout eggs. J. Biol. Chem. **261**, 11550–11557 (1986)
17. Kanamori, A., Inoue, S., Iwasaki, M., Kitajima, K., Kawai, G., Yokoyama, S., Inoue, Y.: Deaminated neuraminic acid-rich glycoprotein of rainbow trout egg vitelline envelope. Occurrence of a novel alpha-2,8-linked oligo(deaminated neuraminic acid) structure in O-linked glycan chains. J. Biol. Chem. **265**, 21811–21819 (1990)
18. Kimura, M., Hama, Y., Sumi, T., Asakawa, M., Rao, B.N., Horne, A.P., Li, S.C., Li, Y.T., Nakagawa, H.: Characterization of a deaminated neuraminic acid-containing glycoprotein from the skin mucus of the loach, misgurnus anguillicaudatus. J. Biol. Chem. **269**, 32138–32143 (1994)
19. Gil-Serrano, A.M., RODRíGUEZ-CARVAJAL, M.A., Tejero-Mateo, P., Espartero, J.L., Thomas-Oates, J., Ruiz-Sainz, J.E., BUENDíA-CLAVERíA, A.M.: Structural determination of a 5-O-methyl-deaminated neuraminic acid (Kdn)-containing polysaccharide isolated from Sinorhizobium fredii. Biochem J. **334**, 585–594 (1998)
20. Campanero, R.M.A., SOLíS, D., Carrera, E., de la Cruz, M.J., DíAZ-MAURIñO, T.: Rat liver contains age-regulated cytosolic 3-deoxy-D-glycero-D-galacto-non-2-ulopyranosonic acid (Kdn). Glycobiology **9**, 527–532 (1999)
21. Dolashka, P., Daskalova, A., Dolashki, A., Voelter, W.: De Novo structural determination of the oligosaccharide structure of hemocyanins from molluscs. Biomolecules. **10**, 1470 (2020)
22. Hardy, S.W., Grant, P.T., Fletcher, T.C.: A haemagglutinin in the tissue fluid of the Pacific oyster, Crassostrea gigas, with specificity for Sialic acid residues in glycoproteins. Experientia. **33**, 767–769 (1977)
23. Tunkijjanukij, S., Giaever, H., Chin, C.C., Olafsen, J.A.: Sialic acid in hemolymph and affinity purified lectins from two marine bivalves. Comp. Biochem. Physiol. B Biochem. Mol. Biol. **119**, 705–713 (1998)
24. Paschinger, K., Wilson, I.B.H.: Anionic and zwitterionic moieties as widespread glycan modifications in non-vertebrates. Glycoconj J. **37**, 27–40 (2020)
25. Du, J., Zhang, Q., Li, J., Zheng, Q.: LC-MS in combination with DMBA derivatization for Sialic acid speciation and distribution analysis in fish tissues. Anal. Methods. **12**, 2221–2227 (2020)
26. Wang, D., Zhou, X., Wang, L., Wang, S., Sun, X.-L.: Quantification of free Sialic acid in human plasma through a robust Quinoxalinone derivatization and LC-MS/MS using isotope-labeled standard calibration. J. Chromatogr. B. **944**, 75–81 (2014)
27. Hu, Z.-X., Cheng, C., Li, Y.-Q., Qi, X.-H., Wang, T., Liu, L., Voglmeir, J.: Recombinant snail Sialic acid aldolase is promiscuous towards aliphatic aldehydes. Chembiochem. (2022). https://doi.org/10.1002/cbic.202200074
28. Laborda, P., Wang, S.Y., Lu, A.M., He, M., Duan, X.C., Qian, Y.J., Jung, Y.S., Liu, L., Voglmeir, J.: Diastereoselective One-Step Synthesis of 2-Keto-3-deoxy-d- glycero-d-galacto-nononic acid (KDN) Analogues as Templates for the Development of Influenza Drugs. Adv Synth Catal **359**, 3120–3125 (2017). https://doi.org/10.1002/adsc.201700678
29. Cao, C., Wang, W.J., Huang, Y.Y., Yao, H.L., Conway, L.P., Liu, L., Voglmeir, J.: Determination of sialic acids in liver and milk samples of wild-type and Cmah knock-out mice. Journal of Visualized Experiments **125**, 56030 (2017)
30. Lyu, Y.M., Li, Y.Q., Song, H.B., Guo, J., Wang, T., Liu, L., Yedid, G., Voglmeir, J.: A Converging Strategy for the Generation of a Virtually Sequenced cDNA Library from Unreferenced Pacific Oysters. Journal of Visualized Experiments **148**, e59462 (2019)
31. Zhang, Y.-Y., Hu, Z.-X., Zhang, S.-Y., Liu, L., Galan, M.C., Voglmeir, J., Ghirardello, M.: Improved ESI-MS sensitivity via an imidazolium Tag (DAPMI-ITag) for precise Sialic acid detection in human serum and CMAH-Null mouse tissues. Anal. Chem. (2025). https://doi.org/10.1021/acs.analchem.5c00752
32. Pabst, M., Grouzdev, D.S., Lawson, C.E., Kleikamp, H.B.C., De Ram, C., Louwen, R., Lin, Y.M., Lücker, S., Van Loosdrecht, M.C.M., Laureni, M.: A general approach to explore prokaryotic protein glycosylation reveals the unique surface layer modulation of an anammox bacterium. The ISME Journal **16**, 346–357 (2022)

33. Kleikamp, H.B.C., Lin, Y.M., Mcmillan, D.G.G., Geelhoed, J.S., Naus-Wiezer, S.N.H., Van Baarlen, P., Saha, C., Louwen, R., Sorokin, D.Y., Van Loosdrecht, M.C.M., Pabst, M.: Tackling the chemical diversity of microbial nonulosonic acids - a universal large-scale survey approach. Chem Sci **11**, 3074–3080 (2020)
34. Pavlova, N.V., Yuziuk, J.A., Nakagawa, H., Kiso, M., Li, S.C., Li, Y.T.: 2-Keto-3-deoxy-D-glycero-D-galacto-nononic acid (KDN)- and N-acetylneuraminic acid-cleaving sialidase (KDN-sialidase) and KDN-cleaving hydrolase (KDNase) from the hepatopancreas of oyster, Crassostrea virginica. J Biol Chem **274**, 31974–80 (1999)
35. Cheng, C., Hu, Z.X., He, M., Liu, L., Voglmeir, J.: Recombinant human N-acetylneuraminate lyase as a tool to study clinically relevant mutant variants. Carbohydrate Research **516**, 108561 (2022)
36. Nakagawa, T., Iwaki, Y., Wu, D., Hane, M., Sato, C., Kitajima, K.: Identification and characterization of a deaminoneuraminic acid (Kdn)-specific aldolase from sphingobacterium species. Glycobiology. **33**, 47–56 (2023)